Role of surface interactions in the dynamics of chiral isopentylcyanobiphenyl mixed with Al_2O_3 powder as studied by dielectric spectroscopy: Numerical analysis

A. Bąk* and K. Chędowska
Rzeszów University of Technology, W. Pola 2, PL-35-959 Rzeszów, Poland
(Received 21 December 2010; revised manuscript received 23 March 2011; published 24 June 2011)

The results of dielectric measurements for a mixture of chiral liquid crystal 5*CB with Al_2O_3 powder are given. A detailed analysis of the dielectric spectra enabled us to obtain information about the influence of the Al_2O_3 grains on the dynamics of the liquid-crystal molecules. Numerical analysis of the results confirmed that the dielectric spectra obtained are complex. In the low-frequency range they are dominated by ionic conductivity while in the whole frequency range two maxima appear. One of them is related to rotations of the molecules around their short axes. In the isotropic phase the corresponding values of the relaxation times are very close to those for bulk 5*CB. Relaxation and conduction processes can be described by a Vogel-Fulcher-Tammann function. In the cholesteric phase, rotation of 5*CB molecules trapped in the pores of Al_2O_3 occurs. Another relaxation process results from dynamics of 5*CB molecules anchoring to Al_2O_3 grains. The temperature dependence of relaxation times related to this process is nonmonotonic.

DOI: 10.1103/PhysRevE.83.061708 PACS number(s): 61.30.−v, 64.70.pp, 68.08.−p, 77.22.Gm

I. INTRODUCTION

In recent years the properties of liquid crystals (LCs) confined in porous matrices have been studied by many authors. Pore shape may be regular (annopore, nuclepore) or more or less random (droplets, sol-gel glasses, or cellulose membranes). Often solid particles are embedded in a liquid crystal. This leads to interactions between the liquid-crystal molecules and the surface of the solid particles. Regions exist where the liquid crystal retains bulk properties, provided the dimensions of these regions exceed 1 μm [1]. In bulk LC, the relaxation processes occurring in different frequency ranges were observed [1–5]. Relaxation processes in the high-frequency region were attributed to molecules rotation around the short axes and libration of the long axes (tumbling). In the isotropic liquid phase the relaxation times of these two processes are comparable but due to the isotropic distribution of molecules impossible to separate of them. In the nematic phase molecules arrangement ceased to be isotropic and both processes were well separated [1,6]. In complex systems (liquid crystals confined in porous materials), other relaxation processes may occur, e.g., the Maxwell-Wagner (MW) relaxation [7]. For nematic isopentylcyanobiphenyl (5CB) in this frequency region, Sinha and Aliev [8] observed an additional, slight, but clearly marked process that they attributed to the rotation of molecules located in the surface layer formed at the pore walls. In the low-frequency region the effects of ionic conductivity can also be observed [9,10].

In this paper the results of dielectric measurements for mixture of chiral isopentylcyanobiphenyl 5*CB liquid crystal containing Al_2O_3 grains are presented. As the grains vary in size (10–300 μ), both bulklike processes and relaxation of anchored molecules in subsurface layers take place. The spatial distribution of grains is random, which means that molecule orientation is arbitrary. Consequently, there are molecules whose orientation is parallel to and others that are perpendicular to the direction of a probing electric field. This results in the superposition of two typical geometries $\vec{E} \parallel \vec{n}$, $\vec{E} \perp \vec{n}$ ($\vec{n}$ is the director).

Relaxation processes were observed in both the isotropic liquid phase and the cholesteric phase in the low- (10^1–10^4 Hz) and high- (10^4–10^7 Hz) frequency regions. With an increase in temperature their absorption maxima diminish and shift toward lower frequencies. Detailed qualitative analysis revealed that the processes observed in the high-frequency region could be attributed to molecules' rotation around their short axes [11]. Comparison of the results obtained for bulk 5*CB and the 5*CB-Al_2O_3 mixture confirm this interpretation [12–14].

Another process observed in the 5*CB-Al_2O_3 mixture at lower frequencies did not occur in the bulk 5*CB. We proved that this low-frequency process is not associated to the MW relaxation. The temperature dependence of the relaxation times of this process shows unusual saddlelike shape. We attributed this relaxation process to the tumbling of the 5*CB molecules anchored to the Al_2O_3 surface. A similar interpretation has been proposed by other authors (cf. Ref. [15]).

In the isotropic phase, we observe a large ionic conductivity. The dependence of the conductivity on relaxation times satisfies the fractional Debye-Stokes-Einstein (FDSE) relation, but the coupling between translational and rotational degrees of freedom is weaker than in the bulk 5*CB.

II. EXPERIMENT

The material studied was a mixture of chiral liquid crystal 5*CB with powdered and porous Al_2O_3. The measurements of the capacitance C (related to ε') and the dielectric loss tangent tgδ (related to ε'') were carried out within the frequency range 100 Hz–40 MHz. They were performed using the Agilent 4294 A precision impedance analyzer with 10% accuracy.

The measuring cell was a brass flat capacitor with circular electrodes 28 mm in diameter and the sample thickness was 0.7 mm. The geometric capacitance of the cell $C_0 = 7.78$ pF was determined with 0.5% accuracy. Temperature was controlled and stabilized using a Lakeshore 331S temperature

*sowa@prz.edu.pl

controller with a platinum sensor Pt100 inserted into the upper electrode.

The sample was heated to 300 K, cooled to 190 K, and then reheated to the initial temperature. The rate of temperature change on cooling was 1.5 K/min, whereas that on heating was 0.5 K/min. The measurements were performed at $\Delta T = 1.5$ K intervals after the desired temperature had been stabilized throughout the sample volume. Temperature was stabilized with 0.1 K accuracy. A detailed description of sample preparation, measurements, and qualitative analysis of results was given in Ref. [11].

Matrices forcing parallel or perpendicular orientation of the molecules in the pores are often used. Preparing such samples does not ensure that in both experiments (i.e., with the molecules parallely or perpendicularly oriented) the volume of liquid crystal filling the pores is the same, having a significant impact on the results obtained. An important advantage of our experiment is that all the results have been obtained for the same sample.

III. RESULTS

The dielectric spectra obtained during cooling and heating of the sample had complex structures [Figs. 1(a), 2(a), and 3]. During cooling, two clearly separated peaks whose height and width depended on temperature [Figs. 1(a) and 2(a)] were seen. The frequencies at which these peaks were observed differed by two or three orders of magnitude. Moreover, in the isotropic liquid phase the effect of ionic conductivity on the spectrum [Fig. 1(a)] was seen. During heating a single but very broad absorption maximum occurred (Fig. 3). The full width at half maximum of the dielectric spectra and their asymmetric shape suggested two overlapping peaks. That is why, for the quantitative description of the dielectric spectra, the superposition of two Havriliak-Negami (HN) [16] functions and the ionic conductivity was used:

$$\varepsilon^*(\omega) = \sum_{k=1}^{2}\left[\varepsilon_{k\infty} + \frac{\Delta\varepsilon_k}{(1+(i\omega\tau_k)^{1-\alpha_k})^{\beta_k}}\right] + i\frac{\sigma}{\varepsilon_0}\frac{a}{\omega^b}, \qquad (1)$$

where $\Delta\varepsilon_k = \varepsilon_k - \varepsilon_{k\infty}$ is the dielectric strength and τ_k is the mean relaxation time of the k-th process. The parameters α_k are Cole-Cole symmetric distribution parameters ($0 \leqslant \alpha \leqslant 1$) and β_k are Cole-Davidson asymmetric distribution parameters ($0 \leqslant \beta \leqslant 1$). For $\alpha = 0$, $\beta = 1$ Eq. (1) reduces to Debye's equation. The parameter σ is the sample conductivity. For ohmic behavior the power $b = 1$, and a is a constant.

After separation of the real and imaginary parts, Eq. (1) may be written as:

$$\varepsilon''(\omega) = \sum_{k=1}^{2}\left[\frac{\Delta\varepsilon_k \sin\beta_k\varphi_k}{\left\{1+2(\omega\tau_k)^{1-\alpha_k}\sin\frac{\pi\alpha_k}{2}+(\omega\tau_k)^{2(1-\alpha_k)}\right\}^{\frac{\beta_k}{2}}}\right] + \frac{\sigma}{\varepsilon_0}\frac{a}{\omega^b}, \qquad (2)$$

$$\varepsilon'(\omega) = \sum_{k=1}^{2}\left[\varepsilon_{k\infty} + \frac{\Delta\varepsilon_k \cos\beta_k\varphi_k}{\left\{1+2(\omega\tau_k)^{1-\alpha_k}\sin\frac{\pi\alpha_k}{2}+(\omega\tau_k)^{2(1-\alpha_k)}\right\}^{\frac{\beta_k}{2}}}\right], \qquad (3)$$

where

$$\varphi_k = \arctan\frac{(\omega\tau_k)^{1-\alpha_k}\cos\frac{\pi\alpha_k}{2}}{\{1+(\omega\tau_k)^{1-\alpha_k}\sin\frac{\pi\alpha_k}{2}\}}, \quad \omega = 2\pi f.$$

Figure 1(a) shows $\varepsilon''(f)$ obtained in the isotropic liquid phase during cooling. The lines result from fitting Eq. (2). There are two distinct, broad maxima shifting toward the lower frequencies as the temperature decreases. In the lowest-frequency region a significant effect of ionic conductivity can be seen. At 300 K $\varepsilon'' \approx 1120$ (not shown in Fig. 2) and it decreases to the value of 29 at 256.5 K. In order to highlight the complexity of the processes the results for the isotropic liquid phase obtained at 258 K and three terms of Eq. (2) have been shown in Fig. 1(b). Figure 1(c) shows the measured values $\varepsilon'(f)$ at 258 K together with fitting Eq. (3).

Ionic conductivity is absent from the cholesteric phase of 5*CB [Fig. 2(a)]; however, two absorption maxima [Fig. 2(b)] and two regions of dispersion [Fig. 2(c)] are still there. On further cooling the maxima move beyond the range of available frequencies. The sample was then cooled to 190 K and transformed to the glassy phase [11]. The calorimetric studies [17,18] show that the sample passes to the glassy phase at 210 K. The dashed lines in Figs. 1(b) and 2(b) represent three processes: I, ionic conductivity; II, an additional process related to tumbling of anchored molecules in subsurface layers; and III, a process due to rotations around the short axes (as in bulk 5*CB).

During heating the glassy phase transforms into the cholesteric phase, but the ε'' values are slightly lower than in the same phase obtained by cooling the sample [Fig. 3(a)]. On further heating, in the temperature range 249 K to 255 K 5*CB crystallizes into the metastable solid phase [11–13]. Figure 3(b) shows the dependence of ε'' on frequency in this phase. The solid lines seen in Fig. 3 were drawn using the parameters obtained from fitting Eq. (2).

Good agreement between the experimental results and the HN function was obtained in the whole temperature range, both when cooling and when heating the sample.

IV. DISCUSSION

The temperature dependence of the relaxation times obtained as a result of fitting the HN function is shown in

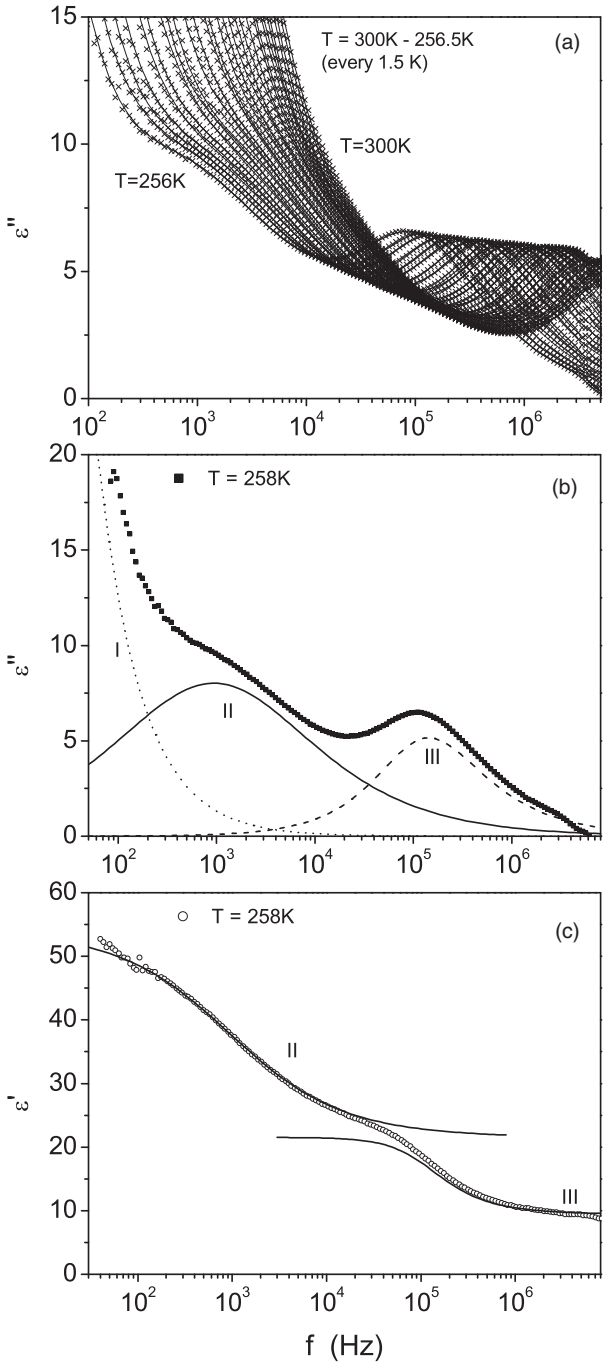

FIG. 1. Frequency dependence of the imaginary (a and b) and real (c) parts of the dielectric permittivity in an isotropic liquid for cooling the sample. The lines result from fitting HN functions which represent the three processes: I, ionic conductivity; II, tumbling of anchored molecules in the subsurface layers; III, molecule rotations around their short axes. In (a) the lines are the sum of these processes.

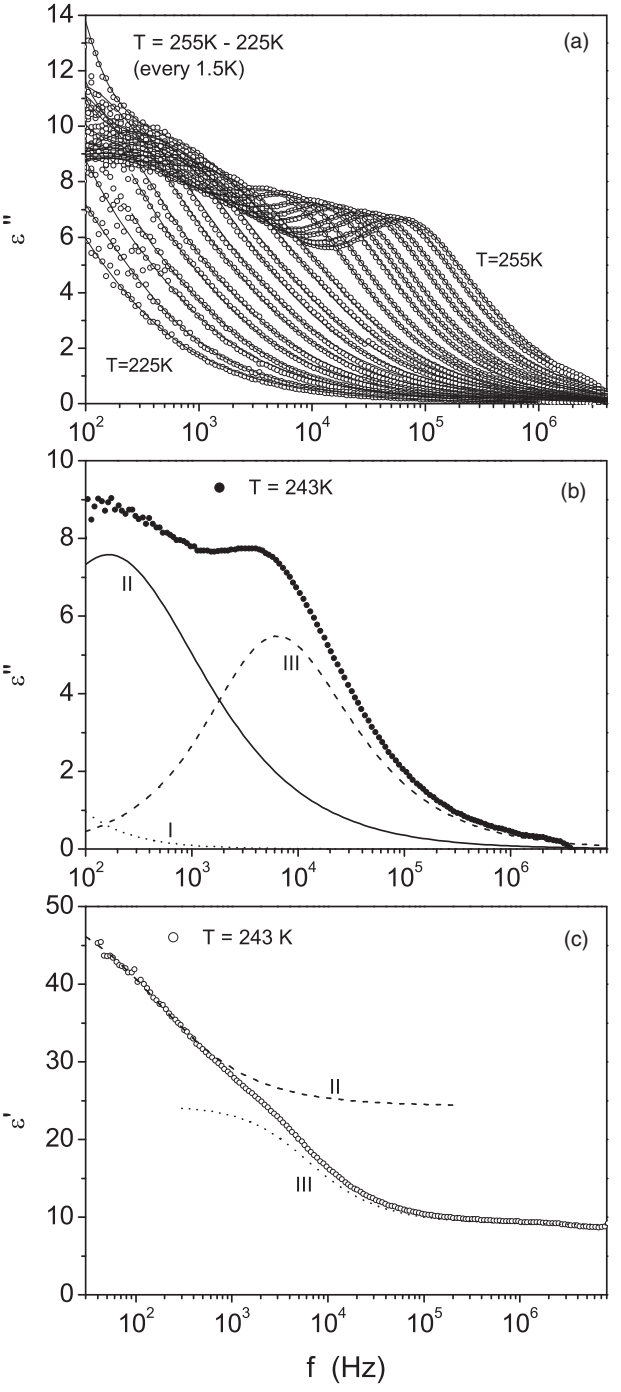

FIG. 2. Frequency dependence of the imaginary (a and b) and real (c) parts of the dielectric permittivity in the cholesteric phase of cooling. The lines show the fit of HN functions for the three processes I (ionic conductivity), II (tumbling of anchored molecules in the subsurface layers), and III (molecules rotations around their short axes). In (a) the lines are the sum of these processes.

Figs. 4 and 5. During cooling two clearly separated relaxation processes (open symbols and crosses) occurred. At the lowest temperatures an additional process was observed. During heating, three relaxation processes (solid symbols) also took place. The relaxation times of two of them did not differ significantly. In the following sections we will try to justify the hypothesis that the relaxation times are related to the rotational and librational motions of the molecules.

A. High-frequency relaxation

The high-frequency process characterized by τ_1 in Fig. 4 has a molecular origin and is related to the rotational motion

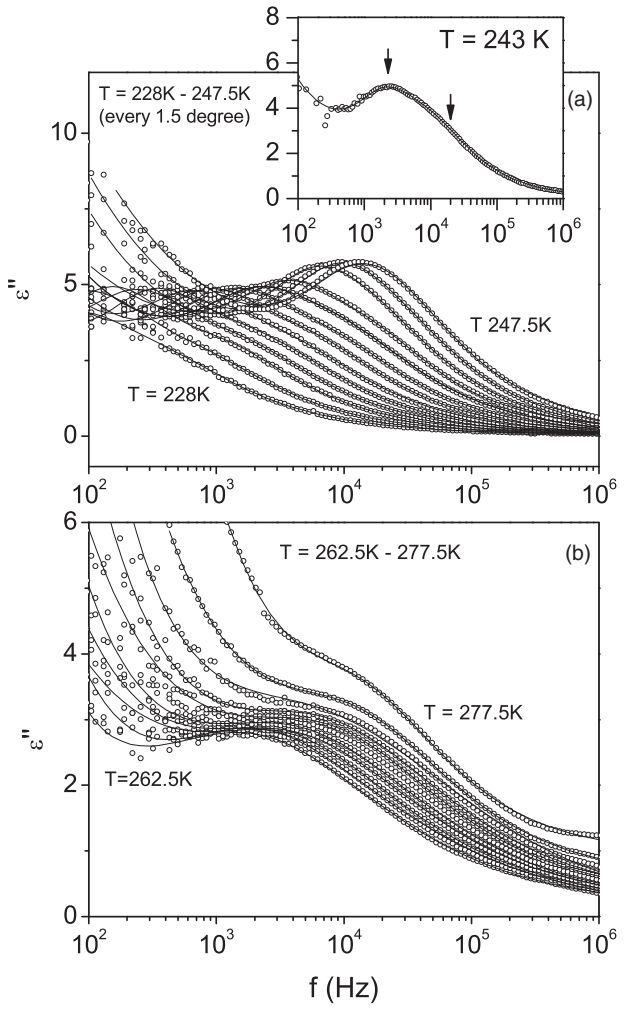

FIG. 3. Dependence of the imaginary part of the dielectric permittivity on frequency in the cholesteric (a) and metastable crystalline (b) phases when heating the sample. The lines show the results of fitting the sum of the two HN functions and ionic conductivity. The complex shape of the dielectric spectrum is clearly visible in the upper panel.

of molecules around their short axes. It is observed in bulk chiral 5*CB [12–14]. The temperature dependence of the relaxation time for the isotropic phase satisfies the Vogel-Fulcher-Tammann (VFT) equation [19–21]

$$\tau_1(T) = \tau_0 \exp\left(\frac{A}{T - T_0}\right), \tag{4}$$

where $A = DT_0$, D is the fragility parameter, τ_0 is the relaxation time for very high temperature, and T_0 is related to a hypothetical, extrapolated ideal glass transition. In Table I the values τ_0, A, and T_0 determined by us and other authors [12,14] are displayed. Our values of these parameters are in good agreement with those obtained by Urban *et al.* [14]. The fragilility parameter equals 5.5. The glass transition temperature T_g calculated from equation(4) for $\tau = 100$ s, $T_g =$ 212 K is in good agreement with the calorimetric data [17,18]. In Fig. 6 we show the fitted results for τ_1 obtained using the VFT equation (4). The linear relationship confirms the correctness of the model used.

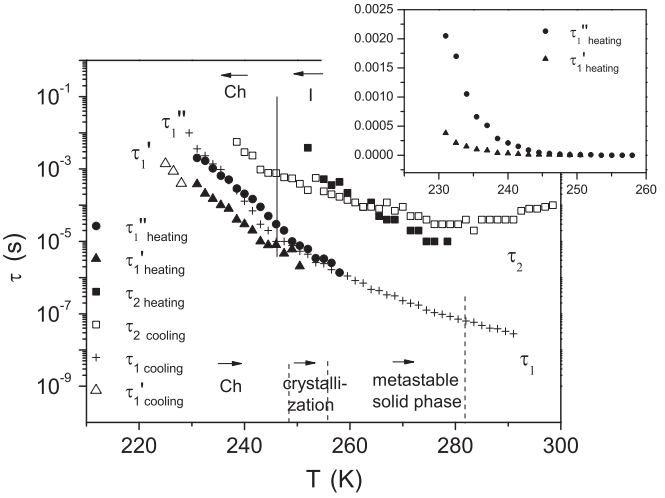

FIG. 4. Temperature dependence of the relaxation times τ for cooling (crosses, open squares, and triangles) and for heating (full squares, triangles, and circles); $\tau_1, \tau_1', \tau_1''$ are related to the molecular rotation around the short axes and τ_2 is related to the tumbling. The times τ_1', τ_1'' tend to the same value as shown in the upper panel.

The results for the cholesteric phase are interesting. During cooling, the sample to 228 K one relaxation time τ_1 (+) was obtained. Then, at this temperature, another process characterized by the relaxation time $\tau_1'(\Delta)$, occurred. Equation (2) yielded two relaxation times during the heating process throughout the cholesteric phase (indicated by full circles and triangles). The complexity of the spectrum shown in the upper panel of Fig. 3(a) also confirms the existence of two relaxation processes. Their relaxations times at 237 K differ by about one order of magnitude. As the temperature increases these times tend asymptotically to the common value 10^{-5} s, although τ_1'' decreases more rapidly than τ_1' (Fig. 4, the upper panel). The asymptotic values of the relaxation times τ_1' and τ_1'' are close to the characteristic time τ_1 therefore they must be related to

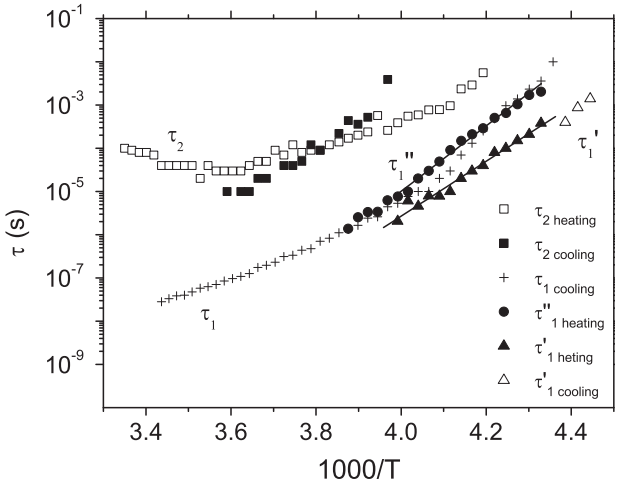

FIG. 5. Dependence of the relaxation times τ on $(1000/T)$ for cooling (crosses, open squares, and triangles) and for heating (full squares, triangles, and circles). The solid lines show the Arrhenius fit to relaxation times for heating with activation energies (121 ± 5) kJ/mol for τ_1' and (145 ± 4) kJ/mol for τ_1''.

TABLE I. Fitting parameters for Eqs. (4) and (7) for 5*CB.

References	Parameters			
	$\tau_0 \times 10^{-12}$ (s)	A (K)	T_0 (K)	σ_0 (Sm^{-1})
[12]	0.32	1347	172	
[14]	4.05	992	182	
Our results, dielectric relaxation	3.78	999	180	
Our results, ionic conductivity		1048	167	5.7×10^{-3}

the rotation of LC molecules around their short axes, whereas the time τ_1 is related to the rotation of free molecules of 5*CB (in the bulk part of the sample).

The activation energy calculated for this process is $E'_{A1} = (121 \pm 5)$ kJ/mol (Fig. 5). As the sample under study was a mixture of 5*CB molecules with the porous Al_2O_3 powder, part of the 5*CB molecules was trapped in the pores of the powder and the time τ''_1 could be ascribed to the rotation of the trapped molecules around their short axes. This interpretation is supported by the results obtained by Aliev *et al.* for nonchiral 5CB [15,22]. They found that the relaxation times associated with the rotation of 5CB molecules around their short axes confined in a porous matrix are one order of magnitude longer than in the bulk material. The activation energy for the rotation of the 5*CB molecules around their short axes in the pores of Al_2O_3 is $E''_{A1} = (145 \pm 4)$ kJ/mol (Fig. 5) which is approximately 20% greater than the activation energy E'_{A1} characterizing bulk 5*CB.

B. Low-frequency relaxation

This process is characterized by a much shorter time τ_2 than the relaxation time associated with the process discussed in the previous section. In the isotropic liquid at 291.5 K the value of this time is about four orders of magnitude shorter than the time τ_1 (Fig. 4). The temperature dependence of τ_2 is weaker than that of τ_1. This process was not observed in bulk 5*CB [12–14], and thus its presence must be associated with the interactions between liquid-crystal molecules and grains

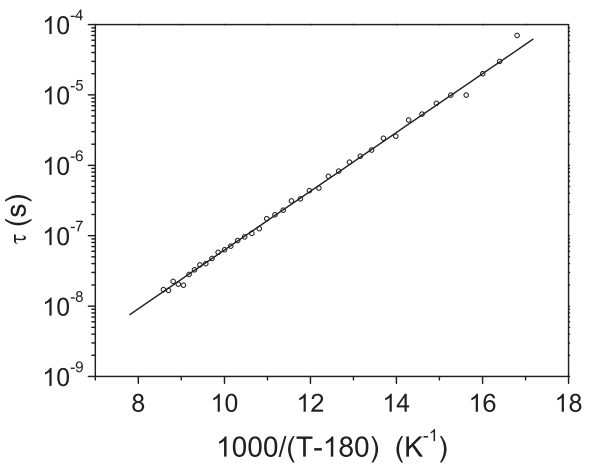

FIG. 6. Fit of the VFT equation to the experimental $\tau_1(T)$ values with the parameters $\tau_0 = 3.78 \times 10^{-12}$ s, $T_0 = 180$ K, and $A = 999$ K.

[23–26]. The temperature dependence of τ_2 is nonmonotonic. It is clearly visible when cooling the sample. Such nonmonotonic (saddlelike) behavior had been observed much earlier both in liquid crystals [27,28] and solids [29]. There are various reasons for these low-frequency processes.

If, in multicomponent mixtures, one of the components has nonzero electric conductivity, the Maxwell-Wagner relaxation takes place [7]. This is related to the accumulation of charges at the interfaces between solid and liquid phases. The formula for the relaxation time resulting from the MW effect, τ_{MW}, was proposed by van Beek [30]

$$\tau_{MW} = 2\pi\varepsilon_0 \frac{2\varepsilon_m + \varepsilon + w(\varepsilon_m - \varepsilon)}{\sigma(1-w)}, \tag{5}$$

where ε_m is the dielectric permittivity of the matrix material (for Al_2O_3 in this case), ε is the dielectric permittivity of the second component (in our case 5*CB), w is the volume fraction of pores, and σ is electric conductivity.

For $\sigma = 6.4 \times 10^{-8}$ Sm^{-1}, $\varepsilon = 12$, $\varepsilon_m = 3$, $w = 0.6$, $\varepsilon_0 = 8.85 \times 10^{-12}$ C^2/Nm^2 corresponding to $T = 270$ K we obtain $\tau_{MW} \approx 0.027$ s. The time $\tau_2 = 1.7 \times 10^{-5}$, so it is more than 100 times shorter than the characteristic time resulting from the MW effect. The distribution parameter of relaxation time for this process $\alpha_2 \approx 0.4$, hence it is not the Debye process. These two facts indicate that the low-frequency process observed in the isotropic phase differs from the MW relaxation.

In the case of the mixture under study the 5*CB molecules can be anchored both within the pores and to the outer surfaces of Al_2O_3. The orientation of the molecules in the subsurface layers depends on such factors as the kind of surface, the method of preparation (e.g., surfactants, radiation, and rubbing), and the thermal history of the sample. For chiral molecules the orientation of liquid crystals also depends on the helix pitch. Most authors indicate that substrate of Al_2O_3 enforces planar orientation of molecules. Planar orientation of molecules on the surface is also typical for the chiral liquid crystals [31–36]. The most probable arrangement molecules 5*CB on Al_2O_3 surface is the one in which the directions of the long axes of the molecules are parallel to the surface. The anchored molecules of 5*CB cannot rotate, whereas the librational motions induced by the alternating electric field can take place. In this process, the decisive role play molecules, with the greatest projections of the dipole moments on the direction of the field.

The nature of changes in relaxation time τ_2 observed during cooling differs from typical activation processes. On lowering the temperature, the rate of this process increases and reaches a maximum value at about 286 K and on further cooling it decreases.

Aliev *et al.* [27] observed similar changes of relaxation time with diminished temperature for the libration of 8CB molecules. The amplitude of these librations depends on temperature. In the ordered phase for which the order parameter $S = 1$, all molecules perform small oscillations and the characteristic time of these movements may be relatively short. With increasing temperature the ordering of molecules reduces ($S < 1$), and they begin motions of increased amplitude requiring longer time.

We assume that in the case of the samples we examined the dynamics is similar. In our case, however, interaction with the surface can greatly affect the arrangement of molecules at the interface of the liquid-crystal and Al_2O_3 surface. In an isotropic liquid at high temperatures the anchored molecules initially have a large unconstrained volume and perform librations characterized by relatively large angles. The relaxation time associated with these movements is quite long. With lowering temperature the energy of the thermal motion of the molecules decreases causing the interaction with the grain surfaces to become dominant and forcing higher molecule ordering. The oscillation amplitude decreases, creating more rapid vibrations. A mathematical description of such nonmonotonic (saddlelike) changes in the relaxation time has been proposed by Ryabov *et al.* [28]:

$$\ln \frac{\tau}{\tau_0} = \frac{E_a}{k_B T} + C \exp\left(-\frac{E_b}{k_B T}\right), \tag{6}$$

where E_a is a potential barrier between two local equilibrium states, E_b is the energy required for participation in relaxation of an inert particle, and k_B is the Boltzmann constant. The last term of Eq. (6) corresponds to Boltzmann's law for the number n of relaxing particles $n = n_0 \exp(-E_b/k_B T)$.

Figure 7 shows the results of fitting equation (6) to the relaxation times obtained for cooling and heating of the sample. The parameter values fitted to this model for cooling are equal $E_a = 66.3 \pm 2.6$ kJ/mol, $E_b = 70.5 \pm 0.2$ kJ/mol, $C = (8.8 \pm 0.3) \times 10^{12}$, $\ln \tau_0 = -39.5 \pm 1.2$. We note that

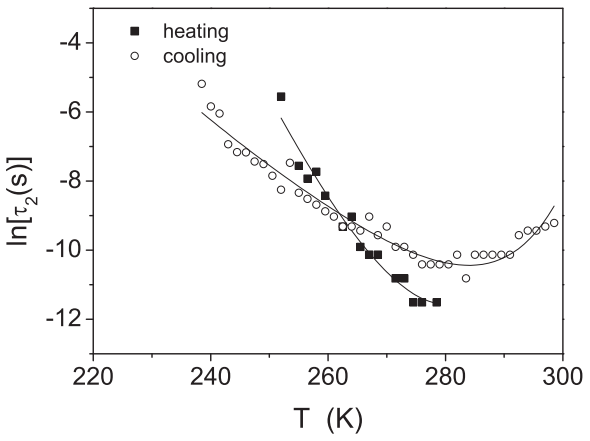

FIG. 7. Temperature dependencies of relaxation times for tumbling of anchored molecules in the subsurface layers during cooling (open circles) and heating (full squares). The solid lines correspond to the fit according to Eq. (6): $E_a = 66.3 \pm 2.6$ kJ/mol, $E_b = 70.5 \pm 0.2$ kJ/mol, $C = (8.8 \pm 0.3) \times 10^{12}$, and $\ln \tau_0 = -39.5 \pm 1.2$ for cooling; $E_a = 170 \pm 19$ kJ/mol, $E_b = 62 \pm 1$ kJ/mol, $C = (9.99 \pm 0.68) \times 10^{11}$, and $\ln \tau_0 = -87 \pm 9$ for heating.

$E_a \approx E_b$. During heating fitting of Eq. (6) gives $E_a = 170 \pm 19$ kJ/mol, $E_b = 62 \pm 1$ kJ/mol, $C = (9.99 \pm 0.68) \times 10^{11}$, and $\ln \tau_0 = -87 \pm 9$. The activation energy E_a is more than twice the energy obtained for cooling. For heating, 5*CB has a different phase polymorphism. The unfreezing cholesteric phase crystallizes into the metastable solid phase. Rotations around the short axes become frozen (Fig. 5) while the librational motions survive in this phase transition. The height of the barrier between the two positions in the metastable solid phase increases. The ability to perform librations remains unchanged and the E_b values during cooling and heating are comparable.

C. Conductivity

In the dielectric spectra obtained, especially in the isotropic liquid, a significant contribution of ionic conductivity is observed. The conductivity coefficient is one of the fitting parameters of Eq. (2). The temperature behavior of conductivity can be reproduced by the VFT-like function [10,37,38]

$$\sigma = \sigma_0 \exp\left(\frac{-A}{T - T_0}\right). \tag{7}$$

The parameters A and T_0, determined from the dependence $\sigma(T)$ shown in Fig. 8, are in good agreement with the values obtained from Eq. (4) (compare Table 1).

The values of the relaxation time $\tau_1(T)$ and conductivity $\sigma(T)$ determined by fitting Eqs. (4) and (7) satisfy the FDSE relation [39–41] that correctly describes the relationship between conductivity and the relaxation time for ordinary liquids as well as for simple glass-forming fluids in a supercooled regime. The relation FDSE can be written as

$$\sigma \tau_1^s = \text{const.}, \tag{8}$$

where s takes values between 0.5 and 0.95 [42] and coupling dc conductivity with dielectric relaxation time, i.e., translational and rotational processes. Small values of s indicate weaker coupling between the translational and rotational motions. For a compound like 5*CB one can expect a linear relationship $\sigma(\tau_1)$. The results shown in Fig. 9 support this conclusion.

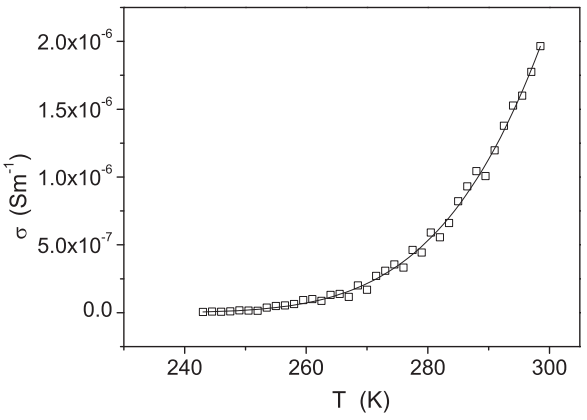

FIG. 8. The fit of the VFT equation to the values of $\sigma(T)$ in the isotropic phase during cooling of the sample. The fitted parameters are $\sigma_0 = 5.7 \times 10^{-3}$ Sm^{-1}, $T_0 = 167$ K, $A = 1047$ K.

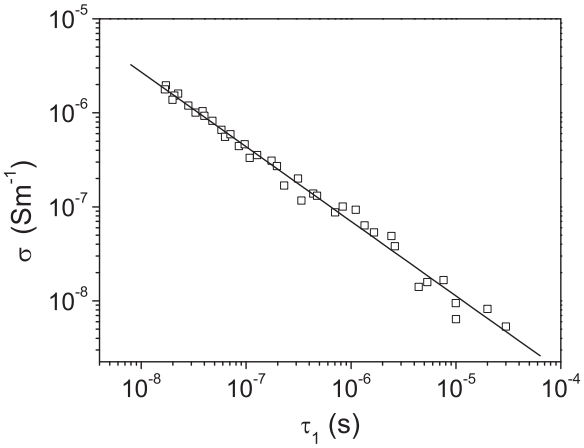

FIG. 9. Linear dependence of σ vs. τ_1 resulting from the FDSE relation, $s = 0.79 \pm 0.01$.

The s value calculated using the least-squares method is comparable with the value 0.77 ± 0.02 obtained by A. Drozd-Rzoska *et al.* for nonchiral 5CB [43] from the FDSE relation.

To describe the relations $\tau(T)$ and $\sigma(T)$ the authors of Ref. [43] used equations resulting from the theory of coupling modes (MCT [44]):

$$\tau(T) = \tau_0^{\mathrm{MCT}}(T - T_{\mathrm{MCT}})^{-\phi},$$
$$\sigma(T) = \sigma_0^{\mathrm{MCT}}(T - T_{\mathrm{MCT}})^{\phi_1}, \quad s = \frac{\phi_1}{\phi}, \tag{9}$$

where T_{MCT} is the ergodic-nonergodic crossover temperature. From equations (9) they obtained the same value of the parameter s as from the FDSE relation. We also fitted the functions (9) to our experimental results.

The values of T_{MCT} calculated from the $\tau_1(T)$ and $\sigma(T)$ dependencies shown in Fig. 4 and Fig. 8 equalled 233 K and 240 K, respectively. The values of the exponents were $\phi_1 = 3.22$, $\phi = 4.37$, and $s = 3.22/4.37 \cong 0.74$. This value is consistent with s obtained from the fit of the FDSE relation (Fig. 9). A. Drozd-Rzoska *et al.* calculated the exponents ϕ and ϕ_1 for bulk 5*CB [45]. They obtained $\phi = 3.6$, $\phi_1 = 3.8$, and $s = 3.6/3.8 = 0.95$. We received a much smaller value of the parameter s for a mixture of Al_2O_3 and 5*CB. This indicates a smaller coupling of the translational and rotational processes than in bulk 5*CB.

The value of T_{MCT} determined by A. Drozd-Rzoska *et al.* [45] for bulk 5*CB based on the temperature dependence of relaxation time and conductivity was 248 K and was in good agreement with the phase-transition temperature determined from calorimetric measurements of $T_{\mathrm{I-Ch}} = 246.6$ K [17,18]. They noted the coincidence between the MCT "critical" temperature and the extrapolated temperature of the hypothetical continuous isotropic-cholesteric phase transition [45].

Both T_{MCT} values determined for a mixture of Al_2O_3 and 5*CB are lower than those obtained for bulk 5*CB. We believe that the addition of Al_2O_3 resulted in reducing the phase-transition temperature, $T_{\mathrm{I-Ch}}$. Such an effect has also been observed by other authors studying the properties of liquid crystals in porous matrices [1,23,26].

The values of T_{MCT} that we calculated based on dependence (9) for a mixture of 5*CB and Al_2O_3 differ by 7 K. Since translational and rotational degrees of freedom in 5*CB and Al_2O_3 mixture are less coupled ($s = 0.74$) they can be retarded at different temperatures. Ionic conductivity in the cholesteric phase disappears and the related translational degrees of freedom are retarded at a higher temperature than the rotational degrees of freedom.

V. CONCLUSION

The numerical analysis reveals a resemblance between the dynamics of the system considered and that of liquid crystals in porous matrices. The response of the system to the probing alternating electric field is the sum of the components coming from 5*CB molecules located both in the region retaining the properties of the bulk material and in the layers at the surface of Al_2O_3. The temperature dependence of the relaxation times in the bulk 5*CB satisfies both VFT and MCT relations equally well.

The temperature T_0 and the parameters A, τ_0, determined from the VFT equation, are comparable with the values obtained by other authors for bulk 5*CB [12,14]. This confirms that the process characterized by the time τ_1 does occur in the bulk material and results from the rotation of molecules around their short axes. The temperature T_0 and the parameter A determined from the dependencies $\tau_1(T)$ and $\sigma(T)$ are comparable.

The T_{MCT} temperature is lower than that determined by A. Drozd-Rzoska *et al.* [45] for bulk 5*CB. We attribute this difference to weaker coupling of the translational and rotational degrees of freedom as indicated by the much smaller value of s for 5*CB with Al_2O_3.

We have proved that the liquid-crystal layer adjacent to the Al_2O_3 surface has properties that differ from those of bulk 5*CB. Liquid-crystal molecules are anchored to the surface and their mobility is restricted to librational movements only. The dependence of the relaxation times on the temperature associated with these movements is nonmonotonic. This dependence is saddlelike in character, during both the cooling and heating of the sample.

The nonmonotonic dependence of relaxation time on temperature was observed in nematic LC, where an increase in the order parameter was related to temperature changes [27,28]. We have shown that a similar dependence of relaxation times can be obtained in the surface layers where appropriate ordering is enforced by interaction with the surface. A slight difference between the energy E_b for cooling and heating indicates that the number of relaxing molecules in the layer is nearly the same in the cholesteric and metastable phases. The librational motions of the molecules in the metastable solid phase are much more constrained, resulting in an increase in the activation energy E_a in this phase.

ACKNOWLEDGMENTS

This work was partially supported by United European grant (ZPORR). We gratefully acknowledge stimulating discussions with Professor T. Paszkiewicz. We thank M. Potoczek for providing the Al_2O_3.

[1] R. Stannarius and F. Kremer, Lect. Notes Phys. **634**, 301 (2004).
[2] M. Arndt, R. Stannarius, W. Gorbatschow, and F. Kremer, Phys. Rev. E **54**, 5377 (1996).
[3] S. Frunza, L. Frunza, A. Schoenhals, H. L. Zubowa, H. Kosslick, H. E. Carius, and R. Fricke, Chem. Phys. Lett. **307**, 167 (1999).
[4] H. Hori, O. Urakawa, and K. Adachi, Macromolecules **37**, 1583 (2004).
[5] S. Pawlus, J. Osinska, S. J. Rzoska, S. Kralj, and G. Cordoyiannis, *Soft Matter under Exogenic Impacts*, edited by S. J. Rzoska and V. A. Mazur (Springer, Berlin, 2007), p. 229.
[6] S. A. Rozanski, R. Stannarius, H. Groothues, and F. Kremer, Liq. Cryst. **20**, 59 (1996).
[7] B. K. P. Scaife, *Principles of Dielectrics* (Clarendon Press, Oxford, 1989).
[8] G. P. Sinha and F. M. Aliev, Phys. Rev. E **58**, 2001 (1998).
[9] O. D. Lavrentovich, V. G. Nazarenko, V. M. Pergamenshchik, V. V. Sergan, and V. M. Sorokin, Sov. Phys. JETP **72**, 431 (1991).
[10] S. Corezzi, S. Capaccioli, G. Gallone, M. Luccesi, and P. A. Rolla, J. Phys. Condens. Matter **11**, 10297 (1999).
[11] A. Bąk, K. Chłędowska, and W. Szaj, Mol. Cryst. Liq. Cryst. **533**, 82 (2010).
[12] M. Massalska-Arodź, G. Williams, I. K. Smith, C. Conolly, G. A. Aldrige, and R. Dąbrowski, J. Chem. Soc., Faraday Trans. **94**, 387 (1998).
[13] M. Massalska-Arodź, G. Williams, D. K. Thomas, W. J. Jones, and R. Dąbrowski, J. Phys. Chem. B **103**, 4197 (1999).
[14] S. Urban, B. Gestblom, and R. Dąbrowski, Phys. Chem. Chem. Phys. **1**, 4843 (1999).
[15] M. R. Bengoechea and F. M. Aliev, J. Non-Cryst. Solids **351**, 2685 (2005).
[16] S. Havriliak and C. Negami, J. Polym. Sci., Part C **14**, 99 (1966).
[17] J. Mayer, M. Massalska-Arodź, and J. Krawczyk, Mol. Cryst. Liq. Cryst. **366**, 211 (2001).
[18] H. Suzuki, A. Inaba, J. Krawczyk, and M. Massalska-Arodź, J. Chem. Thermodyn. **40**, 1232 (2008).
[19] H. Vogel, Phys. Z. **22**, 645 (1921).
[20] G. S. Fulcher, J. Am. Ceram. Soc. **8**, 339 (1923).
[21] M. H. Cohen and G. S. Grest, Phys. Rev. B **20**, 1077 (1979).
[22] F. M. Aliev, M. R. Bengoechea, C. Y. Gao, H. D. Cohran, and S. Dai, J. Non-Cryst. Solids **351**, 2690 (2005).
[23] Ch. Cramer, Th. Cramer, F. Kremer, and R. Stannarius, J. Chem. Phys. **106**, 3730 (1997).
[24] G. Sinha, C. Glorieux, and J. Thoen, Phys. Rev. E **69**, 031707 (2004).
[25] A. R. Bras, M. Dionisio, and A. Schönhals, J. Phys. Chem. B **112**, 8227 (2008).
[26] F. M. Aliev, *Liquid Crystals in Complex Geometries Formed by Polimers and Porous Networks* (Taylor&Francis Ltd, London, 1996).
[27] F. M. Aliev, Z. Nazario, and G. P. Sinha, J. Non-Cryst. Solids **305**, 218 (2002).
[28] Y. E. Ryabov, A. Puzenko, and Y. Feldman, Phys. Rev. B **69**, 014204 (2004).
[29] A. A. Bokov, M. Mahesh Kumar, Z. Xu, and Z. G. Ye, Phys. Rev. B **64**, 224101 (2001).
[30] L. K. H. van Beek, *Dielectric Behavior of Heterogeneous Systems*, Progress in Dielectrics, Vol. 7, edited by J. B. Birks (Heywood, London, 1967), p. 68.
[31] G. Chahine, A. V. Kityk, N. Démarest, F. Jean, K. Knorr, P. Huber, R. Lefort, J. M. Zanotti, and D. Morineau, Phys. Rev. E **82**, 011706 (2010).
[32] R. J. Ondris-Crawford, M. M. Ambrožič, J. W. Doane, and S. Žumer, Phys. Rev. E **50**, 4773 (1994).
[33] M. Ambrožič, and S. Žumer, Phys. Rev. E **59**, 4153 (1999).
[34] H. G. Park, Y. H. Kim, B. Y. Oh, W. K. Lee, B. Y. Kim, D. S. Seo, and J. Y. Hwang, Appl. Phys. Lett. **93**, 233507 (2008).
[35] W. Guo, Ph.D. thesis, Georg-August-Universität Göttingen, 2009.
[36] J. Leys, Ph.D. thesis, Katholieke Universiteit Leuven, 2007.
[37] N. F. Sheppard and S. D. Senturia, J. Polym. Sci., Part B **27**, 753 (1989).
[38] T. Koike and R. Tanaka, J. Appl. Polym. Sci. **42**, 1333 (1991).
[39] F. Stickel, E. W. Fischer, and R. Richert, J. Chem. Phys. **104**, 2043 (1996).
[40] H. Silescu, J. Non-Cryst. Solids **243**, 81 (1999)
[41] S. H. Bielówka, T. Psurek, J. Zioło, and M. Paluch, Phys. Rev. E **63**, 062301 (2001).
[42] S. R. Becker, P. H. Poole, and F. W. Starr, Phys. Rev. Lett. **97**, 055901 (2006).
[43] A. Drozd-Rzoska and S. J. Rzoska, *Metastable Systems under Pressure* (Springer, Berlin, 2010), p. 141.
[44] W. Götze, J. Phys. Condens. Matter **11**, A1 (1999).
[45] A. Drozd-Rzoska, S. J. Rzoska, M. Paluch, S. Pawlus, J. Zioło, P. G. Santangelo, C. M. Roland, K. Czupryński, and R. Dąbrowski, Phys. Rev. E **71**, 011508 (2005).